An Effective Visualization and Analysis Method for Edge Measurement

Andrey Toropov

Rosmark-Steel Co.,
Chelieva street, 13,lit.T, Saint-Petersburg, Russia
toropov@rosmark.ru

Abstract. The terminology burr defines undesirable result of plastic deformation formed in machining process causing degradation of the accuracy and functionality of the product and its assemblies. To supervise the quality of the machined part, effective edge measurement and analysis are necessary. In this paper, we presented a laser-based measurement system including softwares for control and characterisation of burr parameters. Experiments were carried out showing that micro burr around 10 μm and burr formed on a curved surface was successfully measured and analyzed.

1 Introduction

Burr is usually formed around a drilled hole or slitted edge during mechanical machining operations (fig. 1). Burr geometry contains thin and sharp edges which make it difficult to be measured precisely. In contact method, some difficulties are confronted due to the irregular and sharp shape of burr. When height gage is used to measure burr of ductile materials, plastic deformation at the tip of burr reduced the height due to the spring force. When stylus is used, the probe is liable to be broken due to the sharp edge of burr. In this research, non contact method is applied.

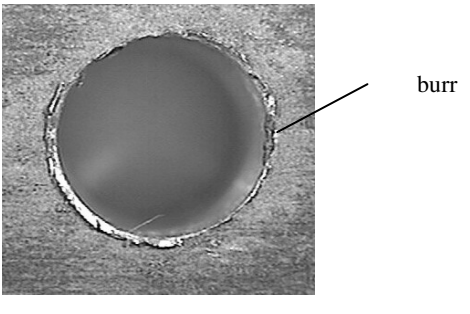

Fig. 1. Burr formed around a drilled hole (microscopic photograph)

It has been shown that the conoscopic holography is the most reliable laser technique for burr measurement in comparison with the triangulation and

O. Gervasi and M. Gavrilova (Eds.): ICCSA 2007, LNCS 4706, Part II, pp. 941–950, 2007.

interferometry methods [1]. Our measurement system is based on this kind of sensor, the Conoprobe sensor. In addition, a precision XY table is equipped for scanning and a software including two modules to control the system and visualise/analyse the data is developed. After digitising process, filtering burr from other components of the surface profile is an important step prior to any numerical characterisation. The robust Gaussian regression filter is successfully applied for separation of burr data and therefore will be introduced briefly in this paper.

2 Specification of the System

2.1 The Connoscopic Holography Method

The conoscopic module is composed of two disc-type polarizers, uniaxial crystals between discs, and CCD as shown in Figure 2.

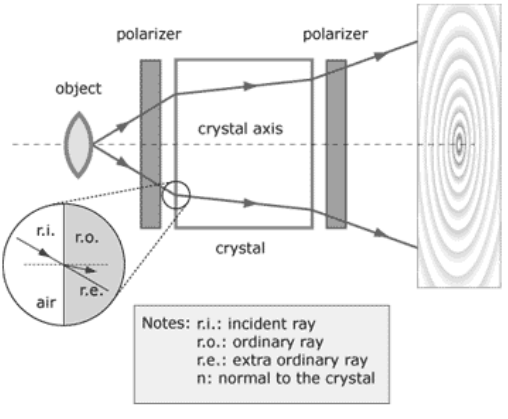

Fig. 2. Schematic of the Conoscopic holography module

The first polarizer disc splits the reflected beam into two orthogonal beams. Each beam passes through the birefringent medium with different velocity due to the different refraction behavior. The second polarizer merges the ordinary beam and extraordinary beam. Phase difference is caused by the difference in velocity due to the different refraction that produces the interference fringe recorded in CCD. The height of the object can be calculated by measuring the diameter of the concentric circle of the interference fringe.

For the Conoprobe sensor, the objective lens can be changed according to precision level. In our experiments, two kinds of lenses with focal lengths of 25 mm and 16 mm are used. Beam spot size, 22μm and 3.5μm respectively, is another main factor affecting measurement accuracy.

2.2 Hardware and Software for Control and Data Acquisition

The measurement system is composed of the sensor, a precise stepmotor xy stage and their controllers connected to a host PC (Fig. 3)

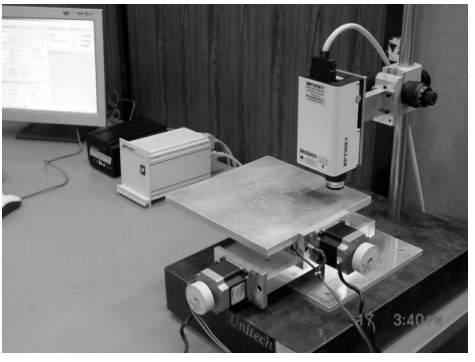

Fig. 3. Photograph of the system

The three-dimensional burr measurement are implemented by a raster scan of the light spot over the measured surface. The stage movements are coded as NC commands by a control software developed in Visual C++.

Each measurement is carried out by a pulse generated inside the Conoprobe sensor controller. This pulse can be defined in two ways, timing or external trigger. In timing mode, it is generated at a preset frequency, while in external signal mode, it is based on an external pulse (usually from a motor's encoder)

A measurement obviously is stabler if it is taken between two consecutive step movements of the motor because vibration is smallest during that time. For this reason, timing method has some drawbacks due to the relative mismatch between the sensor controller timer and that of XY table controller. This also makes the number of acquired points really captured by the sensor inequal to the number of (input) points in each trace. In our system, this error, depending on sampling velocitiy, varies from 0% to 1.2%.

For better synchronization, the external trigger method via direct connection from the table controller to the sensor controller is prefered when accuracy is needed. External pulse is generated by the table controller every "n" steps – where n is the sampling resolution. After the sensor controller received the external pulse, the measurement is set to delay for a small amount of time before it's really carried out to ensure the table completes its instant step (Fig. 4).

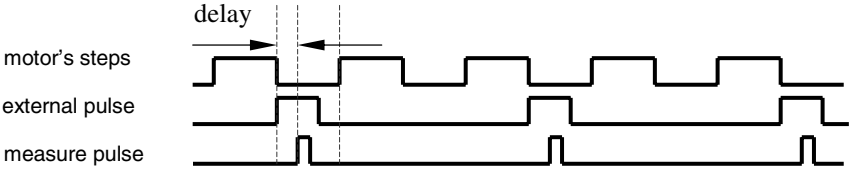

Fig. 4. External pulse from the motor controller triggers measurements

With the control software (Fig. 5) we can define scan parameters : area, feed velocity, sampling rate. It also supports for probe navigation, on-line graphics display and other statistical informations.

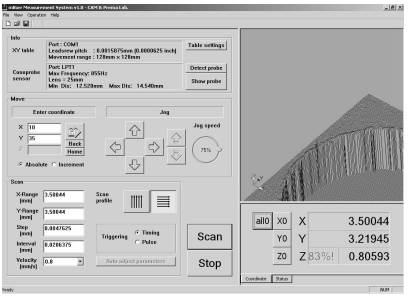

Fig. 5. The control software

3 Analysis Method for Burr Characterization

3.1 Error Removal

Each datum returned from the sensor are the set of 3 values : the digitized height, the Error-bit-set (Ebs) and the Signal-to-noise ratio (Snr) which indicates quality of the signal. In Fig. 6a : the data captured at the time the laser probe scanned across the hole are out of measuring range and might have arbitrary values. Fortunately, they can be identified by their non zero values of Ebs and low values of Snrs (i.e, Snr< 45%) and are set to an equal height to visualise the dept of the hole. However, as can be seen in Fig.3a, errors still remain in the outer region. This implies that Ebs = 0 and Snr > 45% do not guarantee all points are meaningful. Thus, a filter is needed to average such points by their surroundings (Fig. 6b). The filter is constructed by assuming that in the measured surface profile there is no intended feature smaller than a threshold which is input by the user

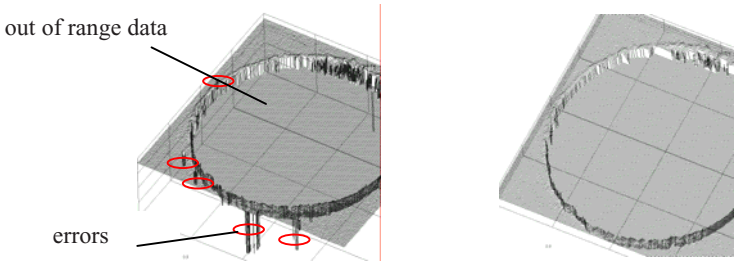

(a) raw data with errors marked with ellipses (b) raw data after filtered

Fig. 6. The first filter to delete errors caused by degradation of signals

3.2 Profile Filtering

Before burr characterization is carried out, the data must go through a second high pass filter that extracts roughness data from the surface profile. The roughness, together with burr are considered as high frequency signals to be separated from the relatively low frequency signal named waviness. However, the existance of the hole where the burr resides around made it impossible to use standardized fiter techniques. The Gaussian filter (ISO 11562) causes distortion at the boundaries and deep valey (here, the edges of hole) of the surface profile while the two step iteration R_k filter (ISO 13565) requires heavy computation and does not fully overcome the distortion problem [2]. Thus, applying these filters will produce a burr higher than its real value. Recently, a filter, namely the robust Gaussian regression (RGR) filter, was developed by Brinkman et al [3] to modify the original Gaussian filter. In RGR algorithm for discrete, the reference waviness is defined as :

$$w(p,q) = \sum_{j1}^{j2}\sum_{i1}^{i2} z(i,j)..\delta_k(i,j).\breve{s}(p-i,q-j). \tag{1}$$

where :

$z(i,j)$: the measured height

$\delta_k(i,j)$: an additional weighting function in the k[th] iteration for robust performance against deep valey, what will be explained later

$\breve{s}(p-i,q-j)$: modified Gaussian weighting function given as :

$$\breve{s}(p-i,q-j) = \frac{s(p-j,q-j)}{\sum_{j1}^{j2}\sum_{i1}^{i2} s(p-i,q-j)} \tag{2}$$

$$s(p-i,q-j) = \frac{1}{2\pi.\lambda c_x.\lambda c_y\Delta_{LP}^2}.\exp\left(-\frac{[(p-i)\Delta x]^2}{2.(\lambda c_x.\Delta_{LP})^2} - \frac{[(q-j)\Delta y]^2}{2.(\lambda c_y.\Delta_{LP})^2}\right) \tag{3}$$

$\Delta_{LP} = \pi^{-1}\sqrt{(\ln 2/2)}$ (constant), λc_x, λc_y are cutoff wavelength in x and y directions.

The differences between this filter and the original Gaussian filter are the function $\breve{s}$ and the introduction of one more coefficient δ_{iter}. From Fig. 7b, it can be seen that the shape of the weighting function $\breve{s}$ is changed at boundaries of the measured area, what is in contrast with the constant shape of the weighting function of the original filter. Thus, the end effects on this filter are compensated.

The additional weighting function δ_k is calculated iteratively. In the first iteration, all δ_1 are set to unity (the non-robust case). In the k^{th} iteration, δ_{k+1} at each point is computed as follow :

$$\delta_{k+1}(i,j) = \left(1 - \left(\frac{r}{C_B}\right)^2\right)^2 \qquad \text{for } \left|\frac{r}{C_B}\right| < 1 \tag{4}$$

$$\delta_k(i,j) = 0 \qquad \text{otherwise}$$

where :

$$r = z(i,j) - w(i,.j) \tag{5}$$

and :

$$C_B = 4.4 \times \text{median}(|z(x,y)-w(x,y)|) \tag{6}$$

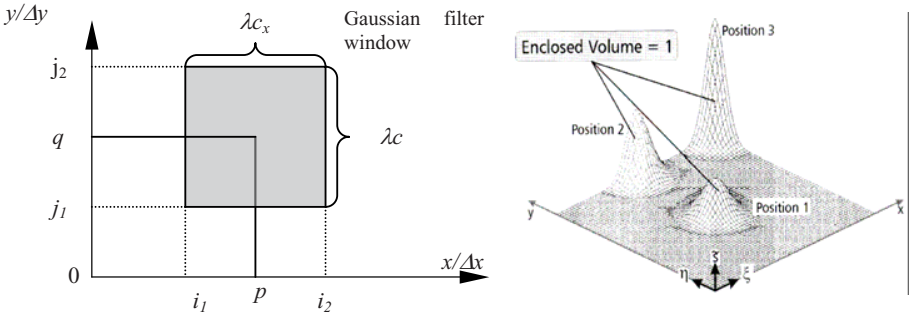

(a) Notations in Eq.(1), (b) Shape of the Gaussian weighting function in RGR filter

Fig. 7. The Gaussian weighting function

As can be seen in eq. (1)&(4), the mean line will be improved through iterations by changing δ_k which is inversely proportional to the difference between r and the scaled median C_B. Thus, the effect of deep valeys on the mean line is gradually reduced. The filter is applied several times.until the change of C_B between two iteration loops is smaller than a given threshold. Finally, the surface roughness (including burrs) is substracted from the profile by eq. (5).

As can be seen in figure 8, the calculated mean line is improved gradually and after 3 iterations, it follows exactly the surface waviness regardless the effects of burr height and the hole depth. The roughness and burr data are then obtained by subtracting the original profile by the calculated waviness. It is shown that the filter works well when burr size is small, no distortion is introduced into the processed profile.

- However, the RGRF filter also has some disadvantages. Similar to other high pass filters, when burr widths in some scan traces are longer than the chosen cut-off wavelength, this large-size burr is unexpectedly filtered. Additionally, the RGRF filter does not follow strictly the form when the surface has large curvatures [4] (fig.9). It also requires excessive computation due to the iterative process, especially when scan points is dense.

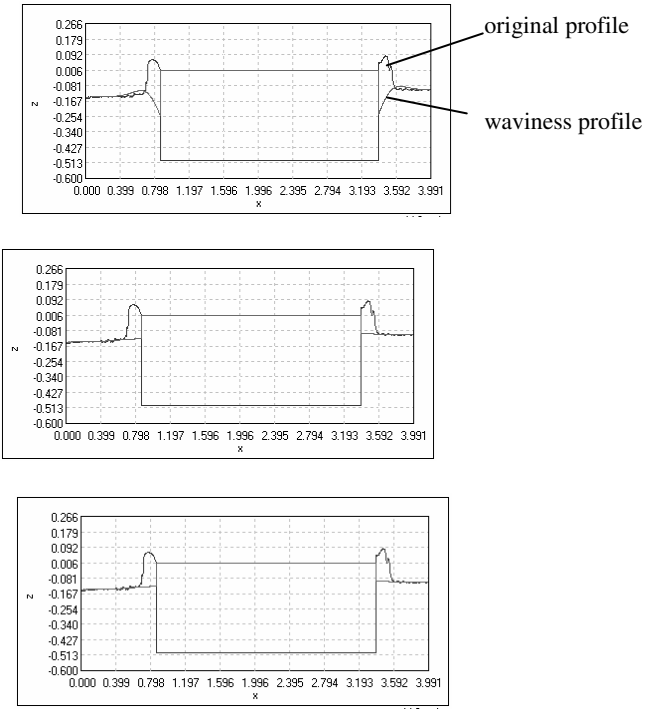

Fig. 8. The filter soon converges after 3 iterations shown from top to bottom

Thus, to increase the efficiency of burr separation, we apply the following scheme :

- if the burr size is large (the effect of waviness and roughness on burr calculation is negligible) and scan surface is an inclined flat surface, we apply the Least square plane fitting to 4 bounday edges to find the mean plane.
- if the burr size is large and scan surface has large curvatures, we apply the RGRF to only four boundary edges. These edges will be used to approximately reconstruct the underlying surface form.
- if the burr size is small, the RGRF is applied to the whole surface.

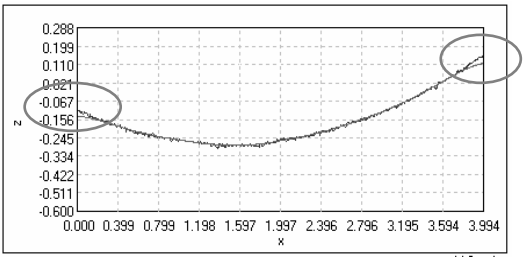

Fig. 9. When surface contains large form, the RGRF cannot remove

3.3 Visualization AND Analysis of Burr Data

The visualization and analysis software was developed in Visual C++ and OpenGL to render the scan data in 2D & 3D graphics (Fig. 10).

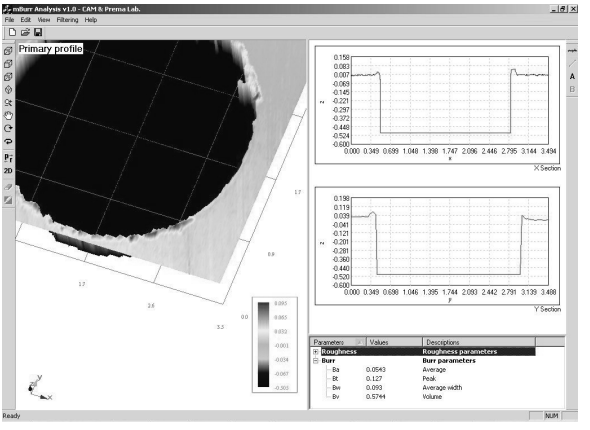

Fig. 10. The analysis software

After filtering, the surface lies horizontally. The point of which height is higher than the average peak roughness R_p is regarded as burr. For more accuracy, it is necessary to do computation restrictively within the region where burr exists. This rectangular region, surrounding the hole, can either be detected automatically or defined by simply dragging the computer mouse over the 3D image.

Output data of the program are maximum and average burr height, burr volume, and burr width which can be added into a database. The surface roughness can also be reported in the case we want to compare the roughness changes before and after a deburring process.

4 Measurement Examples

Burrs were measured and analyzed using the developed burr measurement system. For large burr formed in drilling hole ∅3mm, standard sensor with 25mm focal length was used to scan the area of 3.5mm^2 . Step and interval of the scanning were 0.01mm and 0.02mm, feed rate was 1.27mm/s, scanning time was about 6 mins in timing mode. The 3D image is shown in Fig. 11a.

For micro burrs less than 10μm, high precision sensors with 25mm and 16mm focal lengths were used in pulse triggered mode. Exprimental result on a blanking hole ∅2mm in a 0.3mm thin plate is shown in Fig. 8. Scan parameters are 4mm^2, 1.5μm, 5μm, 0.4mm/s, 15 mins respectively. The average burr height is around 6μm. and burr width is 0.053mm (Fig 11b).

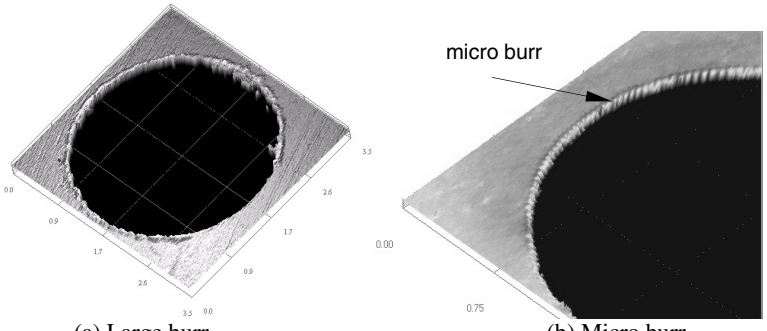

(a) Large burr (b) Micro burr

Fig. 11. Burr on straight surface

Figure 12 and 13 display the results of RGRF on scan surfaces containing large waviness and form. As can be seen in the figures on the left, the base planes are not uniform, which includes the waviness. The burrs along the hole are not well distinguished from the base planes. After filtered as shown in the figures on the right, the plane are very uniform and the burrs are represented clearly.

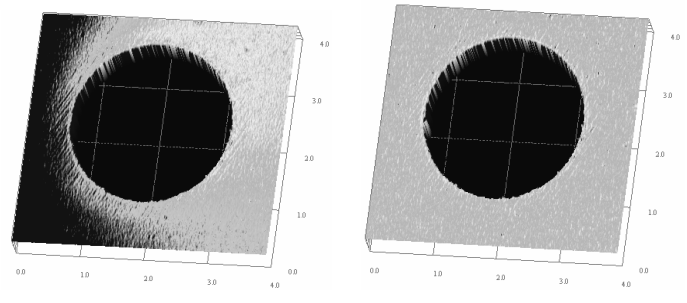

Fig. 12. Burrs formed on a deformed sheet

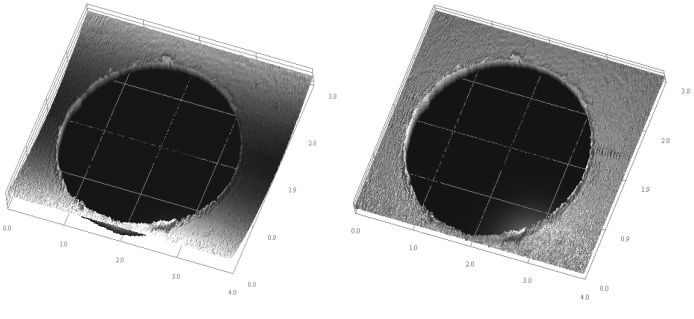

Fig. 13. Burrs on crossing drilled holes

The system failed to measure precisely micro burr less than 4μm due to the effect of residual vibration and laser beam's spot size limit. Also, new system and algorithms to detect micro burrs which has size similar to surface roughness need to be developed.

5 Conclusions

A burr measurement system based on conoscopic holography sensor was developed to measure micro burr automatically and analyze burr geometry. It is shown to be effective in measuring the geometry of sharp edges like micro burrs above 10μm in drilling and fine blanking as well as the burrs formed on curved surfaces. Softwares are built to control the system and calculate the parameters of burr geometry. These parameters will serve as useful information for deciding deburring conditions.

References

1. Ko, S.L., Park, S.W.: Development of an Effective Measurement Method for Burr Geometry. In: Proceedings of 7th Int. Conference on Precision Surface Finishing and Deburring Technology, California, USA (2004)
2. Raja, J., Muralikrishnan, B., Fu, S.: Recent advances in separation of roughness, waviness and form. J. Int. Soc. Precision Eng. and Nanotechnology, 222–235 (2002)
3. Brinkmann, S., Bodschwinna, H., Lemke, H.W.: Development of a robust Gaussian regression filter for three-dimensional surface analysis. In: Proceedings of the Xth International Colloquium on Surfaces, Chemnitz, University of Technology, Chemnitz, pp. 122–132 (2000)
4. Brinkmann, S., Bodschwinna, H., Lemke, H.W.: Accessing roughness in three-dimensions using Gaussian regression filter. Int. J. of Machine Tools and Manufacture 41, 2153–2161 (2001)
5. Press, W.H., et al.: Numerical recipes in C, 2nd edn. Cambridge University Press, Cambridge (1992)